

The Madden-Julian Oscillation

Guy Casella

GFDL – Prof. Chidong Zhang

University of Miami – RSMAS/MPO

FINAL COPY – 29 April 2007

1. Introduction and Background

Discussions among the meteorological community in regard to tropical dynamics rarely exclude the Madden-Julian Oscillation (MJO). Perhaps one of the most widely researched and most published topics throughout the literature, the MJO was discovered over three decades ago by Roland Madden and Paul Julian, for which the phenomenon is named. Utilizing a data set consisting of rawinsonde data from Canton Island (3°S, 172°W), they extracted what appeared to be a strong 40 to 50 day signal in both zonal wind and surface pressure values (Figure 1), which seemed to exist throughout the entire equatorial (tropical) troposphere.

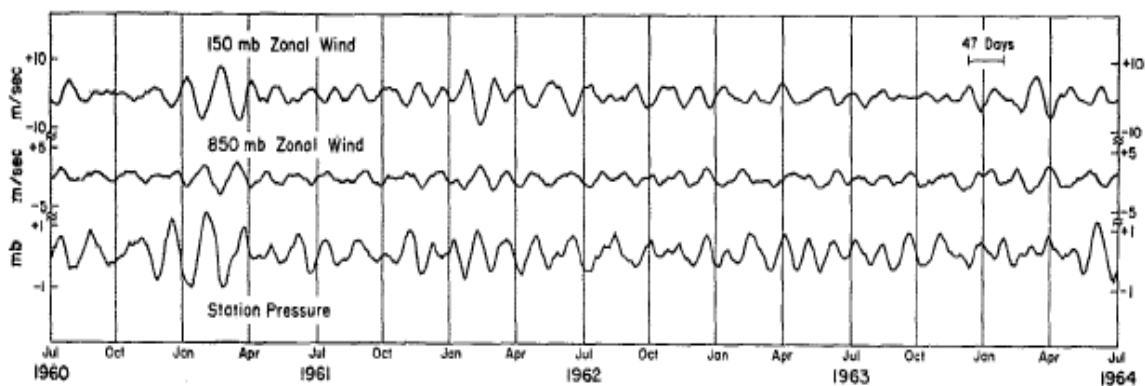


Figure 1: 150mb zonal wind, 850mb zonal wind, and surface pressure observed at Canton; July 1960 to July 1964 (from Madden and Julian, 1971)

Further investigation attempted to link the observations to classic equatorial Kelvin wave theory, and at first, it appeared to be a fairly good match. The signals that led to this included: (1) the observations of the oscillation showed no signal in meridional wind; equatorial Kelvin wave theory assumes $v = 0$ for all motion (Holton and Lindzen, 1968), and (2) the relationship between zonal wind, surface pressure, and tropospheric temperature variations indicate that the system is in geostrophic balance, another fundamental element of the equatorial Kelvin wave. However, it was quickly

noted that other factors negated this theory. Not only did Madden and Julian show that the observed oscillation did not propagate vertically (theory predicts the vertical propagation of equatorial Kelvin waves), it was also proven that the phase speed of the MJO (~ 5 m/s) was much slower than typical values for the phase speed of an atmospheric equatorial Kelvin wave (> 10 m/s). Thus, Madden and Julian concluded that, based on the observations, the oscillation would best be described as a large, zonally oriented circulation cell, rather than as a simple, propagating Kelvin wave. Moreover, they drew the conclusion that moderate to strong convection played a key role in the formulation of the MJO. A future study (Madden and Julian, 1972) unveiled other characteristics of the MJO, namely its eastward propagation and its general north-south limitations (the MJO being equatorially “trapped” between 10°N and 10°S). Here, a schematic featuring these descriptions is offered (Figure 2).

But how correct was the conclusion that the MJO was not bounded by Kelvin wave dynamics, but rather a simple eastward propagating circulation? Section 2 will review equatorial wave theory in order to show that Madden and Julian were, in effect, half correct. Then, we will have established the foundation outlining what the MJO is, allowing the introduction of two main MJO theories for its existence and creation. Section 3 will introduce the theory of the MJO as a response to atmospheric forcing, proceeded by Section 4 which will outline instability in the atmosphere as an alternative theory, with a specific example from Wang and Rui 1990a. Section 5 will present other ideas and variables which interact with the MJO (other theories), as well as an overview, discussion, and some concluding remarks.

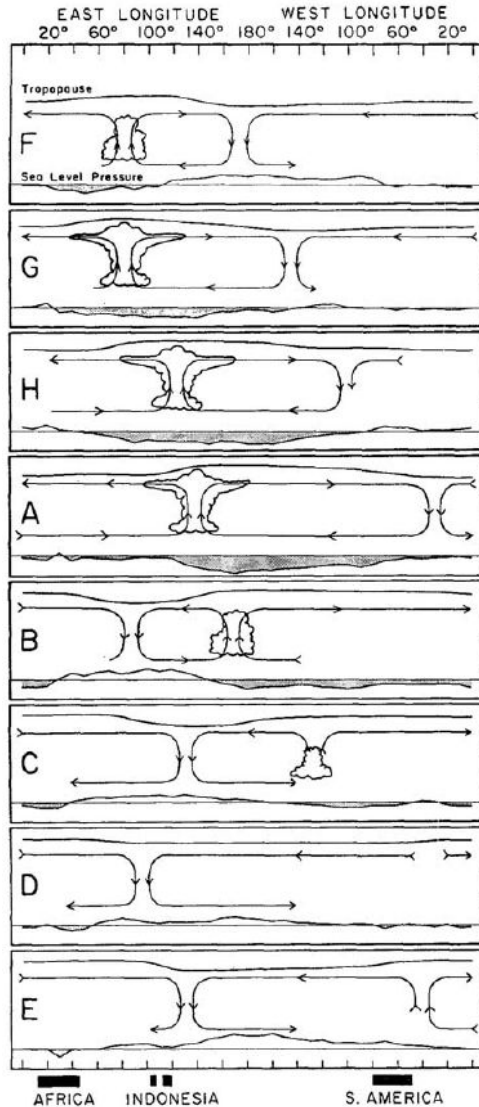


Figure 2: Schematic of the MJO along equator, time increasing downward (from Madden and Julian, 1972)

2. Equatorial Wave Theory in relation to the MJO

In order to better understand equatorial wave dynamics - in the hope of better understanding MJO dynamics - let us consider the following. Matsuno (1966) used the shallow-water model to discern equatorial wave solutions, subject to the beta plane approximation. Using this model, one can derive various classes of equatorial waves. Once done, we will apply observations of outgoing longwave radiation (Wheeler and

Kiladis, 1999) to distinguish the MJO regime in comparison with simple equatorial wave types. Hence, we will see the MJO from a wave standpoint (recall Madden and Julian did not call their oscillation a wave phenomena). Following Matsuno, we will start with the linearized, non-dimensionalized shallow water equations of motion and continuity:

$$\begin{aligned}\frac{\partial u}{\partial t} - fv + \frac{\partial \varphi}{\partial x} &= 0 \\ \frac{\partial v}{\partial t} + fu + \frac{\partial \varphi}{\partial y} &= 0 \quad (1) \\ \frac{\partial \varphi}{\partial t} + c^2 \left(\frac{\partial u}{\partial x} + \frac{\partial v}{\partial y} \right) &= 0\end{aligned}$$

where φ is latitude, f is the Coriolis parameter, and $c = \sqrt{gH}$ is the phase speed of pure gravity waves (H is the mean height of the top surface in our model). We now apply the beta approximation $f = \beta y$, where $\beta = \frac{2\Omega \cos \varphi}{a}$. If we seek zonally-propagating wave solutions to (1) of the form $A = A_0 e^{i(kx - \omega t)}$, we obtain:

$$\begin{aligned}-i\omega u - \beta y v + ik\varphi &= 0 \\ -i\omega v + \beta y u + \frac{\partial \varphi}{\partial y} &= 0 \quad (2) \\ -i\omega \varphi + c^2 \left(ik u + \frac{\partial v}{\partial y} \right) &= 0\end{aligned}$$

Eliminating u and φ from equation set (2) leads to the following second-order differential equation in v :

$$\frac{\partial^2 v}{\partial y^2} + \left(\frac{\omega^2}{c^2} - k^2 - \frac{\beta k}{\omega} - \frac{\beta^2 y^2}{c^2} \right) v = 0 \quad (3)$$

Again, seeking wave solutions of the form $e^{i(kx-\omega t)}$, and applying the boundary conditions $v \rightarrow 0$ as $y \rightarrow \pm\infty$, the following dispersion relationship is obtained:

$$\frac{\omega^2}{c^2} - k^2 - \beta \frac{k}{\omega} = (2n + 1) \frac{\beta}{c}; \quad n = 0, 1, 2, \dots \quad (4)$$

where n is some definite meridional mode. If we solve equation (4) for arbitrary values of k (and applying appropriate assumptions), the dispersion curve diagram of Figure 3 is obtained.

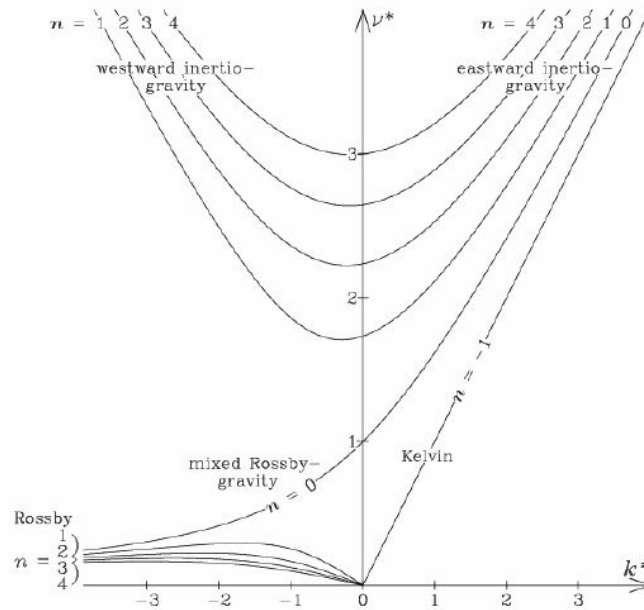


Figure 3: dispersion curve diagram showing solutions of equation (4); here, $v^* \equiv \frac{v}{\sqrt{\beta c}}$ is the nondimensional frequency, and $k^* \equiv k \sqrt{\frac{c}{\beta}}$ is the nondimensional zonal wavenumber (from Wheeler 2003)

Some studies (e.g. Wheeler and Kiladis, 1999) theorized that equatorial wave activity would cause a noticeable feedback in OLR. In fact, it turns out that if the spectral peaks in OLR are overlaid on our dispersion diagram, an interesting result presents itself (Figure 4):

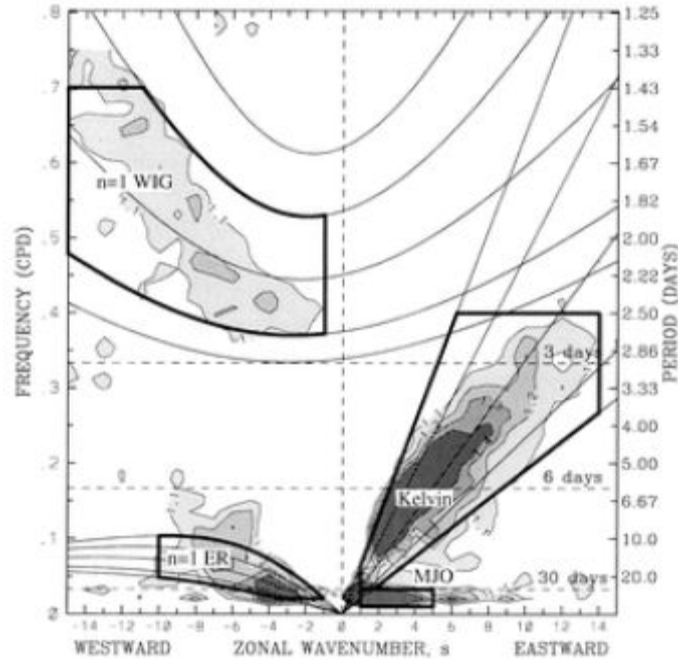


Figure 4: dispersion diagram overlaid with satellite-observed OLR; equatorially symmetric component (from Wheeler 2003)

Here, we note that a distinguishable peak appears away from our “expected” regimes, occurring in the eastward propagation sector, and occurring on the timescale of ~40 days. This, of course, corresponds to the MJO. Hence, we conclude from this study that the MJO is *not* a pure Kelvin wave (as Madden and Julian correctly stated), but rather takes on characteristics of both Kelvin waves *and* Rossby waves.

Many observational studies (e.g. Hendon and Salby, 1994) have proven that the MJO propagates as a mixed Kelvin-Rossby regime early in its life cycle, and then breaks up late in its period, with the Kelvin wave propagating away from the area of convection at greater phase speeds. For observations of the MJO, the reader is referred to Hendon and Salby, 1994, or other outside materials, as the scope of this paper is mainly theoretical.

We have now seen how the MJO has developed from its first discovery to more recent analytical and theoretical study. What has not yet been discussed, however, is

how the MJO itself is created, driven, and sustained over its ~40 day period. Quite frankly, the answer to this question is: we don't know. The MJO has been studied and analyzed for decades, yet still it is unknown exactly how it comes about. Of course, where there is a problem, there are theories in regard to its solution. We will now turn our focus to two of the main theories of the MJO; the MJO as a response to atmospheric forcing, and the MJO as a response to atmospheric instability. For additional material and information, the reader is referred to Zhang 2005 for an overall review of all theories of the MJO.

3. The MJO as a response to atmospheric forcing

3.1 Intraseasonal stationary forcing in the tropics

Since the MJO has its origins in the Indian basin, it has been suggested that its driving mechanism is related to precipitation fluctuations associated with the summer monsoons in Asia and Australia. It was theorized that convection, surface evaporation, and radiation interacted in such a way as to create a ~50 day signal (and thus corresponding to the MJO) in the area of interest (Hu and Randall 1994). In it turned out some studies came to the conclusion that this could be a viable explanation for the MJO. Holland (1986) showed that, for the case of the Australian monsoon, monsoonal bursts occurred on the order of every 40 days. Moreover, Hendon and Liebmann (1990) concluded that the MJO develops in the Australian monsoon self-sufficiently by a 30-50 day modulation of westerly winds.

Of course, it turns out that these theories are invalid. Though the timescales obtained fit the characteristic MJO timescale, their studies and simulations could not

capture any eastward propagating Rossby signal, which as we have seen, is a key aspect of the MJO (Yamagata and Hayashi 1984). Moreover, frictional dissipation/damping will cause any disturbances which result from the forcing to decay as they move away from their source (Lau and Peng 1987). Thus, it is concluded that this theory is an invalid explanation of the MJO.

3.2 Stochastic forcing

Yu and Neelin (1994) showed that a meridional Kelvin wave structure similar to that seen within the MJO could be produced by stochastic (random) mesoscale thermal processes. Other studies (e.g. Salby and Garcia 1987) showed that similar coherent structures could be produced by a stochastic heat source. However, it was also shown that precipitation processes associated with these ideas occurred at spatial scales much smaller than that of the MJO; which as we know, has a deep convective component. Studies generally conclude that, although stochastic forcing plays a critical role in MJO dynamics, it is not a full explanation for the sustainability of the process.

3.3 Lateral forcing

The third theory under this subheading moves away from tropical dynamics and examines the possibility for external (extra-tropical) triggering mechanisms to be a source of the MJO. This so-called “extratropical triggering theory” suggests that MJO cycles are initiated by Rossby wave propagation outside of the tropics, or by energy from baroclinic, mid-latitude eddies extending into tropical (“barotropic”) regimes (e.g. Hsu, et al 1990). However, there exists little evidence that extra-tropical Rossby waves

extend into the upper-level circulation (Kemball-Cook and Weare 2001), which is contrary to the MJO (MJO dynamics fill the depth of the tropical troposphere). Though this seems like another invalid theory, it still stands that this type of forcing provides another stochastic energy source which the MJO may draw off of.

We have seen that all of the theories concerning atmospheric forcing, in general, help to *enhance* the MJO, but are not valid for the explanation of its genesis, propagation, or full dynamical aspects. We will now look at atmospheric instability as a possible theory of the MJO.

4. The MJO as a response to atmospheric instability

Since the MJO carries along with it a strong convective component, it only stands to reason that theories involving atmospheric instability mechanisms must be considered and examined. Here, we will examine two of the more prominent theories: wave-CISK and WISHE. For the case of wave-CISK, we will explore a specific example including frictional effects, as outlined by Wang and Rui 1990a.

4.1 wave-CISK

Based on the idea of CISK (conditional instability of the second kind; refer to Charney and Eliassen, 1964 for details), the wave-CISK (Lindzen 1974) theory proposes that low-level moisture convergence will create deep, cumulus convection. The latent heat processes generated by this will force eastward propagating Kelvin waves, thus inducing additional low-level moisture convergence to the east of the location of the primary convection. At first glance, this would seem to correlate well with

the propagation of the MJO. However, upon further inspection and analysis, the signals created by this process appear to be too weak, and the propagation speeds yielded by most GCMs is much higher (~ 20 m/s \sim Kelvin wave phase speed) than the phase speed of the MJO (recall, ~ 5 m/s) (Lau and Lau 1986).

4.2 Frictional wave-CISK

The result of a faster propagation speed in the wave-CISK applied signal then implies that the addition of some type of frictional forcing could, in theory, account for the differences observed in GCM output. Hence, the “frictional wave-CISK” mechanism as presented by Wang and Rui (1990) is presented here.

This study expands upon a previous study (Wang 1988) which looked at purely Kelvin wave-CISK. Here, a meridional component to the motion is introduced, thus to include Rossby wave propagation in their proposed model. Their “simplified dynamic framework” starts off with the following assumptions:

- The zonal scale is much larger than the meridional scale; acceleration in the v -momentum equation can be ignored. This means that the zonal wind component is in geostrophic balance with the meridional pressure gradient, and the motion is thus semigeostrophic. *This assumption allows inertio-gravity waves, mixed Rossby-gravity waves, and short Rossby waves to be filtered out, leaving only equatorial Kelvin waves and long Rossby waves, which is our main concern here.*
- Non-linear advective terms are ignored, assuming a relatively small zonal velocity scale (here, ~ 4 m/s).

- Assume equatorial beta-plane approximation.
- Specific humidity, q , is given empirically from Wang (1988a) as:

$$q = (0.940 \times SST(^{\circ}\text{C}) - 7.64) \times 10^{-3} \quad (5)$$

where:

$$SST(^{\circ}\text{C}) = SSTMe^{-\frac{\beta y^2}{15C_o}} - \frac{\beta y^2}{C_o} \quad (6)$$

Here, SSTM is the maximum SST at the equator, and C_o is a constant and refers to the wave speed of the gravest baroclinic mode.

Now with these assumptions, the basic equations of motion in pressure coordinates are:

$$\frac{\partial u}{\partial t} - \beta y v = -\frac{\partial \varphi}{\partial x} \quad (7)$$

$$\beta y u = -\frac{\partial \varphi}{\partial y} \quad (8)$$

$$\frac{\partial u}{\partial x} + \frac{\partial v}{\partial y} + \frac{\partial \omega}{\partial p} = 0 \quad (9)$$

$$\frac{\partial}{\partial t} \frac{\partial \varphi}{\partial p} + S(p)\omega = -\mu \frac{\partial \varphi}{\partial p} - \frac{R}{C_p p} Q_c(p) \quad (10)$$

$$\frac{\partial}{\partial t} M'_v + \frac{1}{g} \int_{p_u}^{p_s} \nabla \cdot (q\mathbf{V}) dp = E'_v - P'_r \quad (11)$$

Here, we have the horizontal momentum equations (7 and 8), the continuity equation (9), the thermodynamic equation (10) and the moisture conservation equation (11), where $S(p)$ is a static stability parameter, μ is a coefficient of Newtonian cooling, Q_c is a condensational heating rate per unit mass, M'_v is liquid water path, E'_v and P'_r are the perturbation evaporation and precipitation rates, and p_u and p_s are the pressures at the upper boundary and the surface, respectively. In the case of the moisture conservation

equation, it is assumed that evaporation and precipitation balance, and the total precipitable water does not change with time.

Now that our basic dynamical state has been identified, Wang and Rui go on to apply these foundations to what they call a 2 and ½ layer model, as presented by Figure 5.

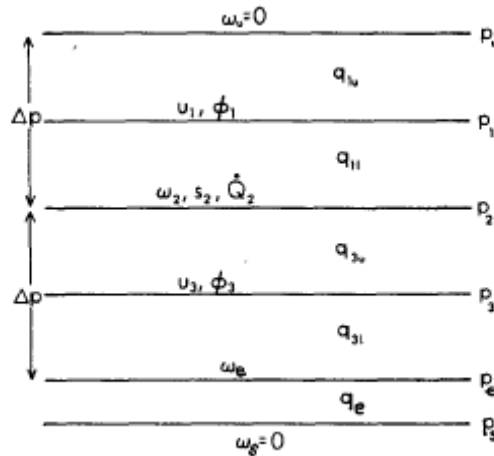


Figure 5: diagram of the 2 and ½ layer model (from Wang and Rui 1990)

This is constructed in order to concentrate on the coupling mechanism of Kelvin and Rossby modes. Here, the upper two layers represent a typical, two-level representation of the atmosphere, and the lower, half level corresponds to a well-mixed boundary layer. This allows for the introduction of the barotropic (velocity independent of height) parts and the baroclinic (velocity of upper level flow is equal and opposite of the low level flow) flow, respectively defined as:

$$u_+ = \frac{1}{2}(u_3 + u_1), \quad v_+ = \frac{1}{2}(v_3 + v_1), \quad \varphi_+ = \frac{1}{2}(\varphi_3 + \varphi_1) \quad (12)$$

$$u_- = \frac{1}{2}(u_3 - u_1), \quad v_- = \frac{1}{2}(v_3 - v_1), \quad \varphi_- = \frac{1}{2}(\varphi_3 - \varphi_1) \quad (13)$$

Applying these to the governing equations yields:

$$\frac{\partial u_-}{\partial t} - \beta y v_- = -\frac{\partial \varphi_-}{\partial x} \quad (14)$$

$$\beta y u_- = -\frac{\partial \varphi_-}{\partial y} \quad (15)$$

$$\frac{\partial u_+}{\partial t} - \beta y v_+ = -\frac{\partial \varphi_+}{\partial x} \quad (16)$$

$$\beta y u_+ = -\frac{\partial \varphi_+}{\partial y} \quad (17)$$

$$\frac{\partial u_+}{\partial x} + \frac{\partial v_+}{\partial y} + \frac{1}{2\Delta p} (\omega_s - \omega_u) = 0 \quad (18)$$

$$\left(\frac{\partial}{\partial t} + \mu\right) \varphi_- + C_o^2 \left(\frac{\partial u_-}{\partial x} + \frac{\partial v_-}{\partial y}\right) = -\frac{R\Delta p}{2C_p p_2} Q_2 - \frac{C_o^2}{2\Delta p} (\omega_s + \omega_u) \quad (19)$$

where ω_s and ω_u are the vertical velocities at the top of the boundary layer and the top of the atmosphere (top of the layer in our model), C_o is again the phase speed of the gravest baroclinic mode with $C_o \equiv \sqrt{\left(\frac{S_2 \Delta p^2}{2}\right)}$ (S_2 is the static stability parameter at p_2), and Q_2 is the condensational heating rate at p_2 defined as:

$$Q_2 = -\frac{bL_C}{\Delta p} [\omega_2 (\bar{q}_3 - \bar{q}_1) + \omega_s (\bar{q}_s - \bar{q}_3)] \quad (20)$$

where b is a moisture factor which accounts for the amount of total moisture convergence which condenses out as precipitation.

As we have seen from our studies in GFD, nondimensionalizing our governing equations proves to be particularly useful. Here, Wang and Rui use the constant C_o as the scaling factor. Using C_o as the characteristic horizontal velocity scale, $(C_o/\beta)^{1/2}$ as the length scale, $(\beta C_o)^{-1/2}$ as the time scale, C_o^2 as the geopotential scale, and

$2\Delta p(\beta C_p)^{1/2}$ as the vertical velocity scale, and applying equation (20), we obtain the following nondimensionalized forms of equations (14) through (19):

$$\frac{\partial u_-}{\partial t} - yv_- = -\frac{\partial \varphi_-}{\partial x} \quad (21)$$

$$yu_- = -\frac{\partial \varphi_-}{\partial y} \quad (22)$$

$$\frac{\partial u_+}{\partial t} - yv_+ = -\frac{\partial \varphi_+}{\partial x} \quad (23)$$

$$yu_+ = -\frac{\partial \varphi_+}{\partial y} \quad (24)$$

$$\omega_e - \omega_u = -\left(\frac{\partial u_+}{\partial x} + \frac{\partial v_+}{\partial y}\right) \quad (25)$$

$$\left(\frac{\partial}{\partial t} + N\right)\varphi_- + (1 - I)\left(\frac{\partial u_-}{\partial x} + \frac{\partial v_-}{\partial y}\right) = \omega_e(B - 1) + \omega_u(I - 1) \quad (26)$$

where the following nondimensional numbers are introduced:

- $N = \mu/\sqrt{\beta C_p}$ is the Newtonian cooling coefficient
- $I = L_e(\bar{q}_3 - \bar{q}_1)/S$ is the ratio of latent heating to adiabatic cooling due to vertical motion at p_2
- $B = L_e(2\bar{q}_e - \bar{q}_3 - \bar{q}_1)/S$ is the ratio of latent heating to adiabatic cooling due to vertical motion at p_e
- $S = 2C_p p_2 C_p^2 / Rb\Delta p$ is the mean static stability

If we now invoke the definition of the vertical velocity at the top of the boundary layer, ω_e , as derived in Wang (1988a), simplified under the semigeostrophic approximation:

$$\omega_e = \frac{(p_e - p_s)E}{2\Delta p(E^2 + y^2)} \left(\frac{2y}{E^2 + y^2} \frac{\partial}{\partial y} - \frac{\partial^2}{\partial y^2} \right) (\varphi_+ + \varphi_-) \quad (27)$$

where E is the Ekman number defined as:

$$E = \frac{\rho_s g A_s}{(p_s - p_b) \sqrt{\beta C_D} h \ln \left(\frac{h}{z_n} \right)}$$

we can see that the governing equations inherently carry a component corresponding to the surface friction as outlined by Ekman dynamics. Since we had been aiming to achieve a model in which surface friction played a role in determining or affecting our surface convergence (and therefore our overall MJO phase speed), we may now apply a set of boundary conditions to our equations. Hence, we will now work to isolate our system of equations into only a baroclinic state, such that they may be implemented in the model. Wang and Rui present two cases, the latter of which representing our goal; however both methods will be discussed here for completeness.

First we will consider the “rigid lid” upper boundary condition, such that

$$\omega_u = 0 \text{ at } p = p_u.$$

In this case, when equation (25) is considered, the horizontal divergence is now balanced by the vertical velocity at the top of the boundary layer (or alternatively, by the compression of air due to frictional mass convergence [Wang and Rui 1990]). However, via equation (26), the baroclinic part, associated with adiabatic cooling or heating and latent heating, as discussed earlier, is also affected. Hence, in this first scenario, both the barotropic and baroclinic parts are coupled via frictional effects. Thus, this is not optimal for the required result of a single set of equations as previously described.

In the second case, the rigid lid is replaced by a “free surface”, so now:

$$\omega_u = \omega_s \text{ at } p = p_u.$$

Now if equation (25) is considered, the divergence of the barotropic part of the flow is equal to zero, and thus all solutions considering barotropic flow is ignored. Hence, we obtain our desired result, and the governing equations (for what is now our purely baroclinic mode) reduce to:

$$\frac{\partial u_-}{\partial t} - yv_- = -\frac{\partial \varphi_-}{\partial x} \quad (28)$$

$$yu_- = -\frac{\partial \varphi_-}{\partial y} \quad (29)$$

$$\left(\frac{\partial}{\partial t} + N\right)\varphi_- + (1 - I)\left(\frac{\partial u_-}{\partial x} + \frac{\partial v_-}{\partial y}\right) = \omega_s(B + I - 2) \quad (30)$$

We note that ω_s still appears in our desired set of equations, and is still defined by equation (27) only now with $\varphi_+ = 0$. Thus, we have arrived at the set of equations, still frictionally dependent, which Wang and Rui implement in their model and compare to the previously discussed pure Kelvin wave-CISK solution (see Wang 1988a, and qualitative description in section 4.1). For comparison and completeness, we should note the frequency obtained for the viscous Kelvin wave-CISK model (Wang 1988a) is given by:

$$\sigma = -\frac{iN}{2} + k^2 \left[(1 - I) - \frac{N^2}{4} + ik \frac{p_s - p_g}{2\Delta p E} (B + I - 2) \right] \quad (31)$$

A similar relationship can be derived for our case (not shown). Wang and Rui go on to show that both Rossby and Kelvin wave modes can be derived using complex eigenvalue/eigenvector analysis, for which the reader is referred to the original paper.

We now have enough information so that the models for both pure Kelvin wave-CISK and Rossby-Kelvin coupled frictional wave-CISK. When the models are

compared, an interesting and potentially desirable result is obtained, as shown below in Figure 6.

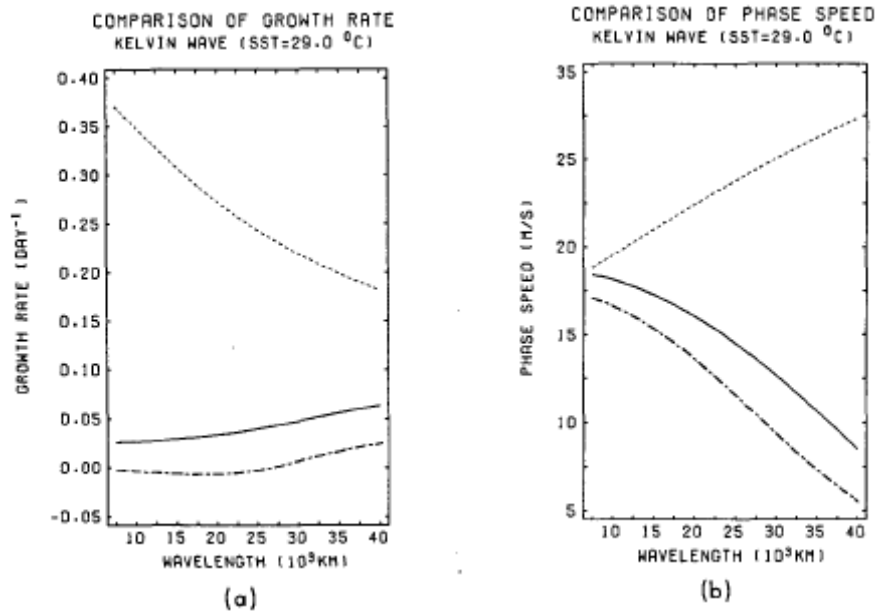


Figure 6: comparison of (a) growth rate and (b) phase speed as a function of wavelength. The dotted line is derived from the pure Kelvin wave-CISK model, the solid and dot-dash lines are derived from the model described above for both uniform SST = 29°C and a latitudinally dependent SST, respectively

Here, we can discern our desired result from our derivations. We see that that phase speed of the pure Kelvin mode increases with increasing wavelength (decreasing wavenumber), and is between 18 and 30 m/s. Alternatively, the phase speed of our mode from the new model *decreases* with increasing wavelength, and is now between 18 and 6 m/s. Therefore as our wavenumber decreases, the phase speed tends more toward the observed phase speed of the MJO. This is a strong suggestion showing that the coupling of Rossby and Kelvin modes tends to slow the propagation of the MJO, which is our ultimate goal.

Other studies (e.g. Chao 1987) have concluded that the coupling between the Rossby and Kelvin wave in the MJO are purely responsible for the slower phase speed, rather than frictional forcing as discussed here.

Along that same train of thought, a study by Seo and Kim (2003) found that Kelvin and Rossby waves left over from previous MJO events also play a role in enhancing convection to the east of the convection core, and suppressing convection to the west of it. They conclude that “frictional Kelvin-Rossby wave-CISK” is a primary factor for the eastward propagation of the MJO, and regard it as “self-generating and self-maintaining through large-scale interactions within the atmosphere” (Marshall and Alves).

In totality, the wave-CISK theory seems the most feasible to this point. Of course, there exist a few studies which regard wave-CISK as unphysical or improbable, but the similarities in results obtained by multiple studies (not all of which were covered here) yields the notion that some of the complex inner-workings of the MJO can be linked directly to this theory. We will now turn to an alternative propagation mechanism of the MJO: WISHE.

4.2 WISHE

The theory of wind-induced surface heat exchange (WISHE; Emanuel 1987) or evaporation-wind feedback (EWF; Neelin et al. 1987) is fairly similar to that of wave-CISK. Here, surface evaporation into the atmosphere is enhanced/reduced by surface easterly/westerly winds to the east/west of a convective anomaly in an easterly mean state (latent heat effects). In the enhancing case, WISHE/EWF acts to increase the total

wind speed to the east of the convective core (as discussed previously), leading to the generation of new convection, while convection becomes suppressed to the west. So, similarly to the wave-CISK case, one will find eastward propagation of the center of convection.

The obvious drawback here is the requirement of mean easterly flow. Unfortunately, flow in the tropical Indian and Pacific oceans is typically *westerly* when the MJO is most prominent. Thus, the WISHE is not as viable of an explanation for the creation of the MJO as wave-CISK may be, as its requirements are not dynamically fulfilled by the ocean or atmosphere at all times of the year.

5. Other factors, discussion, and concluding remarks

We have qualitatively reviewed a few of the major theories of the Madden-Julian Oscillation, all of which failed to provide an adequate explanation for its existence. Because of this, handfuls of other theories exist for the MJO. Here, I will summarize a few of the remaining theories before concluding with discussion and closing comments.

- I. ***air-sea interaction/SST***: SST has a clear role in defining the convective processes which the MJO inherently creates. Higher SST will create deeper convection, and thus may affect the propagation speed of the MJO. However, SST in the equatorial Pacific varies annually and seasonally (ENSO), so a consistent MJO structure would not be observed from event to event.
- II. ***water vapor***: Related to the wave-CISK theory, an increase in water vapor in the area of concern could potentially increase moisture-convergent processes

responsible for the creation of convection in the MJO. Of course, tropospheric moisture content also varies seasonally.

- III. **cloud clusters**: Theories suggest that the MJO may actually be an envelope of “cloud complexes” [*figure to be added here*, Nakazawa 1988] which propagate to the east, embedded in which are individual cloud clusters which propagate *westward*, thereby providing an explanation for the observed mixed Rossby-Kelvin regime. However, most forms of modeling this occurrence typically include *easterly* surface flow, which negates MJO sustainability, as discussed previously.

The Madden-Julian Oscillation is one of the most complex aspects of tropical meteorology. With over three decades of research put into it, dating back to the early 1970's with simple rawinsonde observations, explanations for its existence still have not been found. As we have seen, the factors which contribute to the MJO are many, and are controlled by handfuls of dynamical variables which, until now, have not been resolved by any model, observational, or theoretical analysis.

The theories of the MJO are virtually endless, and to state all of them would require lengthy delving into papers expanding over the course of thirty years. The most prominent of said theories have been presented here, each of which seems to present a viable link to the MJO. Moreover, the frictional wave-CISK theory, as outlined by Wang and Rui 1990a, seems to provide some of the most accurate answers in terms of internal MJO dynamics. However, their respective shortcomings lead us to say that no theory, as of yet, has succeeded in fully resolving the puzzle that is the Madden-Julian Oscillation.

References:

Chao, W. C. (1987), On the origin of the tropical intraseasonal oscillation, *J. Atmos. Sci.*, 44, 1940–1949.

Charney, J. G., and A. Eliassen (1964), On the growth of the hurricane depression, *J. Atmos. Sci.*, 21, 68–75.

Emanuel, K. A. (1987), An air-sea interaction model of intraseasonal oscillations in the tropics, *J. Atmos. Sci.*, 44, 2324–2340.

Hendon, H.H., and B. Liebmann, 1990b: The intraseasonal (30 – 50 day) oscillation of the Australian summer monsoon. *J. Atmos. Sci.*, 47, 2909 – 2923.

Hendon, H. H., M. L. Salby, 1994: The Life Cycle of the Madden-Julian Oscillation. *J. Atmos. Sci.*, 51, 2225 – 2237.

Holland, G.J., 1986: Interannual activity of the Australian summer monsoon at Darwin – 1952-82. *Mon. Wea. Rev.*, 114, 594 – 604.

Holton, J.R., and R. S. Lindzen, 1968: A note on “Kelvin” waves in the atmosphere. *Mon. Wea. Rev.*, 96, 385-386.

Hsu, H.-H., B.J. Hoskins, and F.-F. Jin, 1990: The 1985/86 intraseasonal oscillation and the role of extratropics. *J. Atmos. Sci.*, 47, 823 – 839.

Hu, Q., and D. A. Randall (1994), Low-frequency oscillations in radiative-convective systems, *J. Atmos. Sci.*, 51, 1089–1099.

Kemball-Cook, S., and B.C. Weare, 2001: The onset of convection in the Madden-Julian Oscillation. *J. Climate*, 14, 780 – 793.

Lau, K.-M., and L. Peng (1987), Origin of low-frequency (intraseasonal) oscillations in the tropical atmosphere. Part I: Basic theory, *J. Atmos. Sci.*, 44, 950–972.

Lau, N.-C., and K.-M. Lau, 1986: The structure and propagation of intraseasonal oscillations appearing in a GFDL general circulation model. *J. Atmos. Sci.*, 43, 2023 – 2047.

Lindzen, R. S. (1974), Wave-CISK in the tropics, *J. Atmos. Sci.*, 31, 156–179.

Madden, R.A., and Julian, P.R., 1971: Detection of a 40–50 Day Oscillation in the Zonal Wind in the Tropical Pacific. *J. Atmos. Sci.*, 28, 702 – 708.

Madden, R.A., and Julian, P.R., 1972: Description of Global-Scale Circulation Cells in the Tropics with a 40-50 Day Period. *J. Atmos. Sci.*, 29, 1109 –1123.

Matsuno, T., 1966: Quasi-Geostrophic Motions in the Equatorial Area, *J. Met. Soc. of Jpn.*, 44, 25-42

Neelin, J. D., I. M. Held, and K. H. Cook (1987), Evaporation-wind feedback and low-frequency variability in the tropical atmosphere, *J. Atmos. Sci.*, 44, 2341–2348.

Salby, M. L., and R. R. Garcia (1987), Transient response to localized episodic heating in the tropics. Part I: Excitation and short time, near-field behavior, *J. Atmos. Sci.*, 44, 458–498.

Seo, K.-H., and K.-Y. Kim, 2003: Propagation and Initiation mechanisms of the Madden-Julian Oscillation, *J. Geo. Res.*, 108, Art. No. 4384.

Wang, B., 1988a: Dynamics of tropical low frequency waves: An analysis of moist Kelvin waves. *J. Atmos. Sci.*, 45, 2051-2065.

Wang, B., and H. Rui, 1990a: Dynamics of the coupled moist Kelvin-Rossby wave on an equatorial beta-plane. *J. Atmos. Sci.* 47, 397-413.

Wheeler, M., 2003: Equatorial waves. *Encyclopaedia of the Atmospheric Sciences*, 2313– 2325.

Wheeler, M., and Kiladis, G.N., 1999: Convectively Coupled Equatorial Waves: Analysis of Clouds and Temperature in the Wavenumber–Frequency Domain. *J. Atmos. Sci.*, 56, 374 – 399.

Yamagata, T., and Y. Hayashi (1984), A simple diagnostic model for the 30–50 day oscillation in the tropics, *J. Met. Soc. Jpn.*, 62, 709–717.

Yu, J.-Y., and J. D. Neelin (1994), Modes of tropical variability under convective adjustment and the Madden-Julian Oscillation. Part II: Numerical results, *J. Atmos. Sci.*, 51, 1895–1914.

Zhang, C. (2005), Madden-Julian Oscillation, *Rev. Geophys.*, 43, RG2003, doi:10.1029/2004RG000158.